Title

Tracing nitrate sources and transformations using △17O, δ 15N, and δ 18O-NO3 − in a coastal plain river network of eastern China

Authors

Ji, Xiaoliang
Shu, Lielin
Li, Jian
et al.

Publication Date

2022-07-01

DOI

10.1016/j.jhydrol.2022.127829

Peer reviewed

Journal of Hydrology 610 (2022) 127829

Contents lists available at ScienceDirect

Journal of Hydrology

journal homepage: www.elsevier.com/locate/jhydrol

Research papers

Tracing nitrate sources and transformations using $\triangle^{17}O$, $\delta^{15}N$, and $\delta^{18}O\text{-}NO_3^-$ in a coastal plain river network of eastern China

Xiaoliang Ji [a], Lielin Shu [a], Jian Li [a], Congyuan Zhao [a], Wenli Chen [a], Zheng Chen [a,c], Xu Shang [a,c], Randy A. Dahlgren [d], Yue Yang [b,c,*], Minghua Zhang [a,d,*]

[a] Key Laboratory of Watershed Science and Health of Zhejiang Province, School of Public Health and Management, Wenzhou Medical University, Wenzhou 325035, China
[b] Zhejiang Provincial Key Laboratory for Water Environment and Marine Biological Resources Protection, College of Life and Environmental Science, Wenzhou University, Wenzhou 325035, China
[c] Southern Zhejiang Water Research Institute (iWATER), Wenzhou 325035, China
[d] Department of Land, Air and Water Resources, University of California, Davis, CA 95616, USA

ARTICLE INFO

This manuscript was handled by Huaming Guo, Editor-in-Chief, with the assistance of Mahmood Sadat-Noori, Associate Editor

Keywords:
Nitrate sources
Stable isotopes
^{17}O anomaly
Wen-Rui Tang River
SIAR

ABSTRACT

Identifying the sources and transformations of riverine nitrate plays a critical role in mitigating nitrogen enrichment of river networks. Several previous studies have used $\delta^{18}O\text{-}NO_3^-$ to quantitatively assess riverine nitrate contributed by atmospheric nitrate and terrestrial sources, but their results have great uncertainty due to the wide range of $\delta^{18}O\text{-}NO_3^-$ values and isotopic fractionation during nitrogen-cycling processes in terrestrial environment. The nitrate ^{17}O anomaly ($\triangle^{17}O\text{-}NO_3^-$), as an unambiguous tracer of atmospheric nitrate, is a promising tool to effectively separate atmospheric nitrate from microbially produced nitrate. However, to our knowledge, $\triangle^{17}O\text{-}NO_3^-$ approach has not been previously applied to identify nitrate pollution sources in plain river networks of eastern China. In this study, we used a multiple isotope approach ($\delta D/\delta^{18}O\text{-}H_2O$ and $\delta^{15}N/\delta^{18}O/\triangle^{17}O\text{-}NO_3^-$) for the first time to quantitatively identify sources and transformations of riverine nitrate in a hypereutrophic coastal plain river network namely Wen-Rui Tang River located in eastern China, which is a region receiving high inputs of atmospheric nitrogen deposition. The $\triangle^{17}O\text{-}NO_3^-$ values in precipitation and river water during the study period (April–June of 2021) varied from 14.83‰ to 31.39‰ and from − 2.82‰ to 9.66‰, respectively. The $\delta D/\delta^{18}O\text{-}H_2O$ values revealed that river water mainly originated from recent precipitation with little evaporation. Moreover, the $\delta^{15}N/\delta^{18}O\text{-}NO_3^-$ values indicated that microbial nitrification, not denitrification, was the predominant nitrogen-cycling process in the watershed. Based on a Bayesian mixing model (Stable Isotope Analysis in R, SIAR) using $\delta^{15}N/\triangle^{17}O\text{-}NO_3^-$, municipal sewage was identified as the dominant nitrate source (50.5 ± 11.7%), followed by soil nitrogen (23.8 ± 13.7%), atmospheric nitrate deposition (14.3 ± 2.9%), and nitrogen fertilizer (11.4 ± 8.7%). Finally, an uncertainty analysis for nitrate source apportionment demonstrated that the greatest uncertainty was associated with soil nitrogen, followed by municipal sewage, nitrogen fertilizer, and atmospheric nitrate deposition. This study provides important scientific information on riverine nitrate source apportionment to guide pollution control/remediation strategies and highlights the benefits of utilizing $\triangle^{17}O\text{-}NO_3^-$ to enhance nitrate source apportionment.

1. Introduction

Coastal plain zones, which are occupied by 70% of the word population, are characterized by intensive anthropogenic activities (Narvaez-Montoya et al., 2022). Nitrate contamination in aquatic ecosystems is a serious and enduring global environmental problem that is especially pronounced in many coastal plain zones. Nitrate contamination should be addressed as the water quality is becoming degraded such that the water cannot be used for drinking water (via desalination) and industrial or agricultural activities (Panagopoulos, 2021, 2022). High nitrate

* Corresponding authors at: Zhejiang Provincial Key Laboratory for Water Environment and Marine Biological Resources Protection, College of Life and Environmental Science, Wenzhou University, Wenzhou 325035, China (Y. Yang). Key Laboratory of Watershed Science and Health of Zhejiang Province, School of Public Health and Management, Wenzhou Medical University, Wenzhou 325035, China (M. Zhang).
E-mail addresses: yangyue2018@wzu.edu.cn (Y. Yang), mhzhang@ucdavis.edu (M. Zhang).

https://doi.org/10.1016/j.jhydrol.2022.127829
Received 3 January 2022; Received in revised form 26 March 2022; Accepted 10 April 2022
Available online 15 April 2022

concentrations may increase biological productivity and ultimately lead to altered phytoplankton communities and increased seasonal anoxia/hypoxia, as well as potential risks to human health (e.g., "blue baby" syndrome, thyroid disorders, stomach cancer, diabetes, and miscarriage) (Burow et al., 2010; Ostad-Ali-Askari et al., 2017; Shang et al., 2020). Nitrate concentrations in river networks are controlled by the interplay between allochthonous pollution sources and multiple interacting nitrogen biogeochemical transformations. Nitrate originates from a wide array of sources, including atmospheric nitrate deposition (AD), nitrogen fertilizer (NF), soil nitrogen (SN), livestock excreta, and municipal sewage (MS). Similarly, many nitrogen cycling processes (e.g., plant/microbial uptake, ammonia volatilization, nitrification, and denitrification) affect the form and concentrations of several nitrogen species (Zhang et al., 2019; Ostad-Ali-Askari and Shayannejad, 2021). To effectively control and remediate nitrate pollution, it is imperative to trace and understand the factors controlling the fates and sources of nitrate in a watershed.

During the past few decades, analytical techniques for stable isotopes of nitrate ($\delta^{15}N$, $\delta^{18}O\text{-}NO_3^-$) have improved considerably. A major advance was the development of the "denitrifier method" for the dual analyses of the N/O isotopes of nitrate (Sigman et al., 2001; Casciotti et al., 2002). Determination of nitrate isotopes using the denitrifier method is easier and quicker than previous methods (e.g., ion-exchange, cadmium-azide reduction, and $AgNO_3$ method). Consequently, $\delta^{15}N/\delta^{18}O\text{-}NO_3^-$ are frequently used to assess nitrate sources and transformations (Ji et al., 2017; Biddau et al., 2019; Ostad-Ali-Askari et al., 2019; Torres-Martínez et al., 2020, 2021b; Wu et al., 2021). The theoretical concept for the dual-isotope approach is the characteristic $\delta^{15}N$ and $\delta^{18}O\text{-}NO_3^-$ values of nitrate originating from different pollution sources (Paredes et al., 2020). For instance, $\delta^{15}N\text{-}NO_3^-$ from AD, NF, SN, and MS varies from − 13‰ to 13‰, −6‰ to 6‰, 0‰ to 8‰, and 4‰ to 25‰, respectively (Kendall and McDonnell, 1998; Xue et al., 2009). Further, the $\delta^{18}O\text{-}NO_3^-$ of AD ranges from 25‰ to 75‰, which are appreciably higher than those derived from nitrate fertilizer (17‰ to 25‰) and nitrification of NF, SN, and MS ($\delta^{18}O\text{-}NO_3^-$ = −10‰ to 15‰) (Chen et al., 2020; Mayer et al., 2001). However, $\delta^{18}O\text{-}NO_3^-$ cannot completely distinguish between the origin of nitrate from AD and nitrification or nitrate fertilizer because of the wide range of $\delta^{18}O\text{-}NO_3^-$ in AD and isotopic fractionation effects on ^{18}O from nitrogen-cycling processes. In order to overcome this limitation, a promising nitrate ^{17}O anomaly ($\triangle^{17}O\text{-}NO_3^-$) has been employed as a tracer of atmospheric nitrate deposition (Michalski et al., 2003).

In the atmosphere, mass-independent isotopic fractionation occurs when ozone (O_3) is formed resulting in the $\delta^{17}O\text{-}O_3$ value being significantly greater than the expected value according to $\delta^{18}O\text{-}O_3$. This phenomenon is termed an "isotopic anomaly" and can be expressed as $\triangle^{17}O = \delta^{17}O - 0.52 \times \delta^{18}O$ (Xia et al., 2019). Nitrate derived from atmospheric deposition is characterized by anomalous ^{17}O enrichment given that ^{17}O-enriched O_3 is transferred to nitrate during NO_x oxidation (Michalski et al., 2004). The $\triangle^{17}O\text{-}NO_3^-$ of AD is positive and is generally reported within the range of 17‰ to 35‰. Conversely, the majority of terrestrial nitrogen-cycling processes, such as nitrification and denitrification, are mass-dependent fractionation processes, which leads to $\triangle^{17}O\text{-}NO_3^-$ derived from terrestrial sources being close to 0‰. $\triangle^{17}O\text{-}NO_3^-$, as an unambigous tracer, was employed to identify nitrate sources in several studies. For example, Liu et al. (2013) used triple nitrate isotopes to determine that unprocessed atmospheric nitrate accounted for 0–7% of nitrate in the Yellow River (China). Similarly, Hundey et al. (2016) applied $\triangle^{17}O$, $\delta^{15}N$, and $\delta^{18}O\text{-}NO_3^-$ to apportion the sources of nitrate at Uinta Mountain (Utah, USA), and they found that at least 70% of nitrate in aquatic systems originated from anthropogenic-derived atmospheric deposition. Xia et al. (2019) investigated the $\triangle^{17}O\text{-}NO_3^-$ values of the Yellow River and Changjiang River source regions located in the Qinghai-Tibetan Plateau. They found that atmospheric sources contributed 10 ± 4% of riverine nitrate in the Qinghai-Tibetan Plateau and the $\triangle^{17}O\text{-}NO_3^-$ values in rainwater (average value = 16.4‰) were lower than those reported for low-elevation regions (19–30‰). In eastern China, AD pollution is a serious issue because of the intensive anthropogenic activities including agricultural activities and fossil fuel combustion during recent decades, which leads to a dramatic increase in the emission of reactive nitrogen (Zhu et al., 2015; Liu et al., 2016). For the Wen-Rui Tang River watershed, Liao et al. (2015) estimated the nitrate flux from the atmosphere to be 13–32 kg NO_3^--N/ha·yr, which confirms the AD might be an important riverine nitrate source. Therefore, conducting additional research is highly warranted to advance the application/interpretation of $\triangle^{17}O\text{-}NO_3^-$ for differentiating/quantifying nitrate pollution sources in surface waters of eastern China. However, until now, the application of $\triangle^{17}O\text{-}NO_3^-$ to nitrate source apportionment remains very limited. Little is known regarding the detail characteristics of $\triangle^{17}O\text{-}NO_3^-$ in rainwater and river water of eastern China. To the best of our knowledge, $\triangle^{17}O\text{-}NO_3^-$ approach has not been previously applied to identify nitrate pollution sources in plain river networks of eastern China.

In view of the above considerations, this study aims to: (1) investigate the characteristics of $\triangle^{17}O\text{-}NO_3^-$ in river water and rainwater of a coastal plain river network of eastern China; (2) identify the fates/transformations of nitrogen at the watershed scale; and (3) determine the proportional contributions of the various nitrate pollution sources using isotopic analysis in combination with a Bayesian-based stable isotope mixing model (SIAR model) based on $\delta^{15}N/\triangle^{17}O\text{-}NO_3^-$. This study provides a process-level understanding of nitrate pollution at the watershed scale and improves the accuracy of nitrate source apportionment. The novelty of this study is the application of $\triangle^{17}O\text{-}NO_3^-$ for tracing riverine nitrate sources in eastern China for the first time, which will provide some new insights into riverine nitrate source contributions for developing effective nitrate pollution control strategies.

2. Materials and methods

2.1. Study area

The Wen-Rui Tang River watershed (27°51'–28°02' N, 120°27'–120°46' E) is situated in rapidly developing Wenzhou City of eastern China (Fig. 1) where has >2 million people living in the urban zone and a total population of ~ 9 million (Liao et al., 2021). The Wen-Rui Tang River is a representative plain river network, covering an area of ~ 740 km^2 with 75% located in a flat alluvial plain (elevations = 3.0–4.2 m). The main stem length is ~ 34 km and an extended tributary network of ~ 1200 km with many hardened waterways. The forest land is mainly located on high elevations of the hills whereas the built (including residential and industrial) and agriculture lands are distributed to low elevations of the alluvial plain. Forest and built lands are the dominant land-use types, accounting for ~ 40% and ~ 38% of the entire watershed area. Residential land with the central to northern area containing Wenzhou city center is densely populated with intensive commercial and services activities. Light industries including electroplating, hardware, shoe and leather industries are the predominant industrial types within the watershed. At present, ~100% of the industrial effluents are collected and treated (Wenzhou Municipal People's Government, 2020). Agricultural land covers ~ 20% of the watershed area with staple crops being fruits (e.g., melons, oranges, and bayberry), vegetables, soybeans, sweet potato, rice, tea, and flower gardens. The application rates of nitrogen fertilizer are ~ 300 kg N/ha, and the most commonly used nitrogen fertilizers for local farmers are ammonia-based composite fertilizers and urea. Climate is subtropical monsoon with annual rainfall, precipitation days, and temperature of 1800 mm, ~160 days, and 18 °C, respectively. Rainfall is concentrated (~70%) during the period from April to September. River flows are nearly quiescence for much of the year due to the plain topography, except when gates to the Ou River are open for releasing flood water during storm events (e.g., typhoons) or occasionally for flushing heavily polluted waters during the dry season. Owing to rapid urbanization and industrial/agricultural

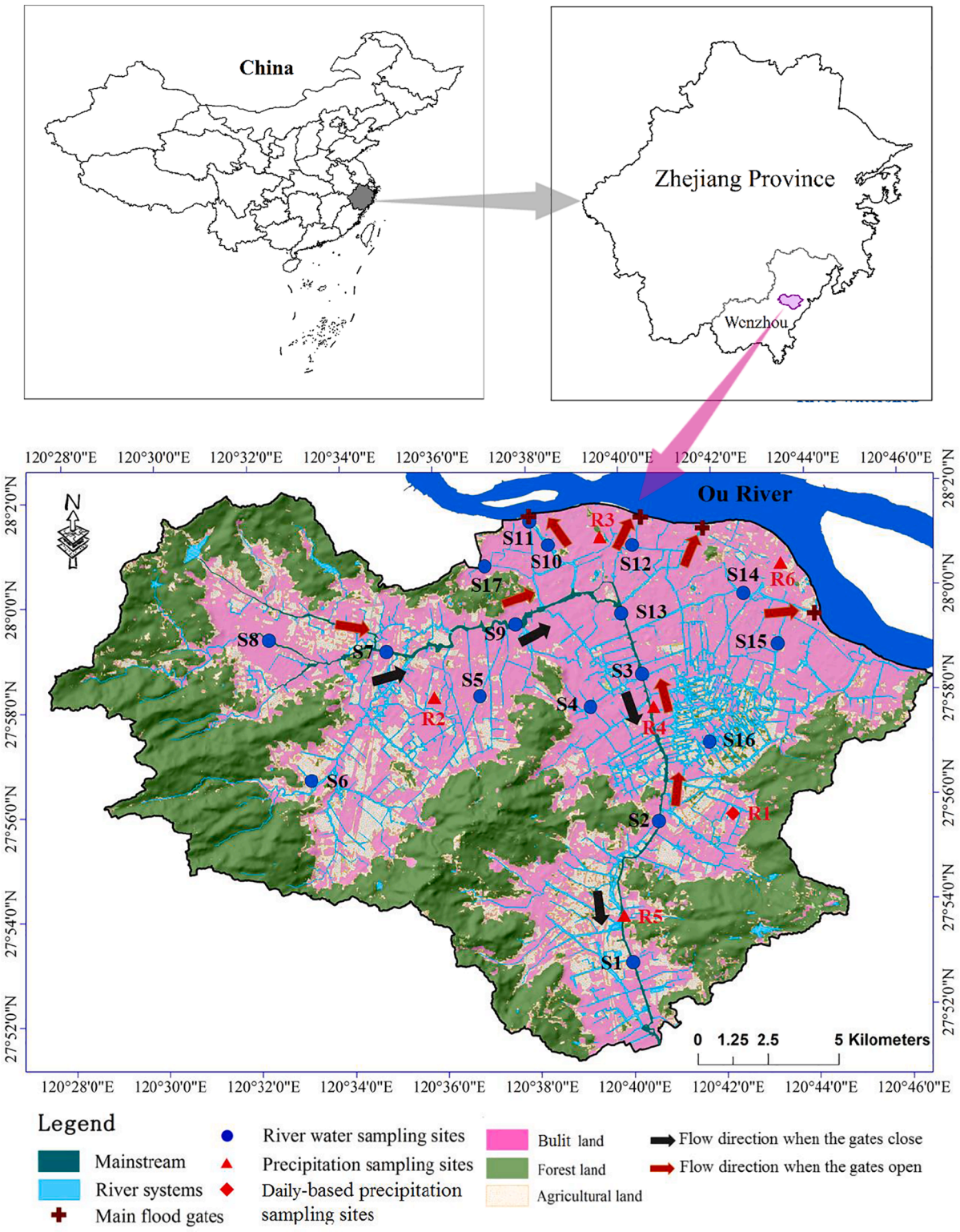

Fig. 1. Map showing sampling sites and major land-use categories in the Wen-Rui Tang River watershed.

development of Wenzhou beginning in the 1980s, water quality in the Wen-Rui Tang River was seriously deteriorated. Since 2015, a series of water resource protection practices such as relocation of livestock/poultry breeding farms, strict ban on factory effluent discharge to river, removal of river sediments, improvement in the sewage collection, and establishment of sewage treatment facilities have been implemented to improve water quality, especially to address eutrophication.

2.2. Sampling and analysis

River water was collected from 17 sites distributed along the Wen-Rui Tang River and its tributaries (Fig. 1). Three river water sampling campaigns were performed in April, May, and June of 2021, and a total of 51 river water samples were collected. We specifically choose the wet season (April, May, and June) because it depicts a time period when the entire watershed is contributing water and associated nitrogen to the

river network, which provides a representative snapshot of watershed-scale nitrogen sources. For each river water sampling event, field parameters such as water temperature (T), dissolved oxygen (DO), pH, electrical conductivity (EC_{25} °C), and chlorophyll *a* (Chla) content were recorded directly in situ using a multi-parameter water-quality sonde (YSI-EXO2, Xylem, USA). At the same time, river water was collected using an organic glass hydrophore sampler from a 30 cm depth in the center of the stream segment. The collected river water samples were immediately stored in pre-cleaned 0.5 L high density polyethylene bottles and subsequently placed in a foam box with ice packs.

To acquire isotopic signatures of potential pollution sources, samples of rainwater, soil, and nitrogen fertilizer were also collected within the watershed. Specifically, a total of 38 rainwater samples were collected using a funnel/bottle collector on a daily basis. Among the 38 rainwater samples, 28 samples were collected at one site in our university (site R1, Fig. 1) throughout the study period of April–June 2021, and the other 10 samples were collected at twice rainwater sampling events conducted from additional five monitoring sites (sites R2–R6, Fig. 1) in May and June. Owing to funding constraints, 24 representative samples were selected from the 38 rainwater samples for analysis of isotopic composition. A total of 32 surface soil samples were collected in agricultural/forest lands within the watershed at depth of 10 cm using a shovel. Ammonium salts (N-P-K compound fertilizers, n = 7) and urea (n = 3), as the major nitrogen fertilizer, were purchased from the local market.

In the laboratory, half of each rainwater and river water sample was filtered through a 0.45 μm mixed cellulose ester membrane filter (Tengjin, Tianjin, China) to remove large particulates within 12 h. Filtered samples were used for determination of dissolved ion concentrations and stable isotope compositions, while non-filtered water samples were used for total nitrogen (TN), total phosphorous (TP), and total organic carbon (TOC). Filtered and non-filtered samples were then stored at − 20 °C prior to completion of analyses within seven days.

Nutrient concentrations were analyzed colorimetrically with a continuous-flow analyzer (Autoanalyser-3, Seal, Germany), and each sample was determined in duplicate. The following colorimetric methods were applied: salicylate method for NH_4^+-N, hydrazine reduction method for NO_3^--N, sulfanilamide/N-1-naphthylethylene method for NO_2^--N, the molybdenum-antimony method for PO_4^{3-}-P, alkaline potassium persulfate digestion combined with hydrazine reduction method for TN, and potassium persulfate digestion combined with molybdenum-antimony method for TP. Furthermore, ion chromatography (Compact IC plus 882, Metrohm, Switzerland) was used for chloride (Cl^-) determination, and a total organic carbon analyzer (TOC-L, Shimadzu, Japan) was utilized for TOC determination. Cl^- and TOC of each sample were determined in duplicate. Detection limits were TN/TP = ~0.02 mg N or P/L, NH_4^+-N/NO_3^--N/NO_2^--N/PO_4^{3-}P = ~0.003 mg N or P/L, Cl^- = ~0.1 mg Cl/L, and TOC/TC/IC = ~0.1 mg C/L.

The $\delta^{15}N$, $\delta^{17}O$, and $\delta^{18}O$-NO_3^- values of each sample were analyzed using the bacterial denitrifier method at the Institute of Applied Ecology, Chinese Academy of Sciences (Shenyang, China). Nitrate was transformed to gaseous nitrous oxide (N_2O) by denitrifying bacteria called *Pseudomonas aureofaciens* (ATCC 13985, United States), which naturally lack the reductase activity of N_2O. Subsequently, the N_2O was analyzed for $\delta^{15}N$, $\delta^{17}O$, and $\delta^{18}O$ by trace gas pre-concentrator coupled to isotope ratio mass spectrometry (IsoPrime PrecisION, IsoPrime Ltd., U.K.). The analytical precision of the $\delta^{15}N$, $\delta^{17}O$, and $\delta^{18}O$-NO_3^- values were ± 0.3‰, ±0.5‰, and ± 0.6‰, respectively. $\triangle^{17}O$-NO_3^- values were calculated as $\triangle^{17}O\text{-}NO_3^- = \delta^{17}O\text{-}NO_3^- - 0.52 \times \delta^{18}O\text{-}NO_3^-$. For $\delta D/\delta^{18}O$-H_2O analyses, H_2O was first converted into CO and H_2 at 1280 °C. The resulting H_2 and CO were respectively measured for δD-H_2O and $\delta^{18}O$-H_2O on a water vapor isotope analyzer (Picarro L2140-I, Picarro, USA) at the Chinese Academy of Agricultural Sciences (Beijing, China). The analytical precision of δD-H_2O and $\delta^{18}O$-H_2O were ± 3‰ and ± 0.2‰, respectively. Nitrogen fertilizer and soils were dried, homogenized, and ground to pass a 149-μm nylon screen. The powdered samples were acidified with 0.5 M HCl and rinsed to a neutral pH with deionized water. Nitrogen in the fertilizer/soil samples was reduced to N_2 by high temperature combustion by Elementar Element Analyzer, and then, the $\delta^{15}N$ values of the resulting N_2 was determined *via* isotope ratio mass spectrometry (IsoPrime 100, IsoPrime Ltd., U.K.). The analytical precision for $\delta^{15}N$ was ± 0.2‰. Replicate standard samples were determined at ~ 10 sample intervals during the isotopic composition analyzed in the lab to ensure that the isotopic data are of high quality and reproducibility. Stable isotope ratios were expressed as delta (δ) notation by referring to the deviations in per mil (‰) relative to the international standards as follows:

$$\delta(‰) = \left(\frac{R_{sample}}{R_{standard}} - 1\right) \times 1000 \quad (1)$$

where R_{sample} and $R_{standard}$ are the isotope ratios (i.e., $^{15}N/^{14}N$, $^{17}O/^{16}O$, $^{18}O/^{16}O$ and $D/^{1}H$) of the samples and standards. The standards for N isotope and the other isotopes (i.e., $\delta^{17}O/\delta^{18}O$-$NO_3^-$ and $\delta D/\delta^{18}O$-H_2O) are N_2 in air and Vienna Standard Mean Ocean Water, respectively.

2.3. Bayesian isotope mixing model

The proportional contributions of multiple potential nitrate sources were calculated using a Bayesian isotope mixing model known as Stable Isotope Analysis in R (SIAR) model based on $\delta^{15}N/\triangle^{17}O$-$NO_3^-$. SIAR model, which is an open-source software package within the R computing program (https://cran.rproject.org/web/packages/siar/index.html), is proposed to estimate the proportional contributions of end-members (i.e., different sources) to a mixture (Parnell et al., 2010). In the model framework, end-members are considered as random variables characterized by a probability function, and the Dirichlet distribution is the prior contribution of proportional contribution. Considering that the analytical forms of posterior distribution of the proportional contribution are difficult to determine, the SIAR model employs Markov Chain Monte Carlo method for generating a large amount of realizations for characterizing proportional contribution of each end-member. The SIAR model assumes that the stable isotopic values and fractionation factor of nitrate sources follow a normal distribution; as such, it necessitates the use of the mean value and standard deviation of isotopic signatures and fractionation factor of each nitrate pollution source as model inputs. The key benefit of using SIAR model is that it allows users to analyze the uncertainties associated with the source apportionment problem (Ju et al., 2022). The model can be expressed as follows:

$$X_{ij} = \sum_{k=1}^{k} P_k\left(S_{jk} + C_{jk}\right) + \varepsilon_{ij} \quad (2)$$

$$S_{jk} \sim N\left(\mu_{jk}, \omega_{jk}^2\right) \quad (3)$$

$$C_{jk} \sim N\left(\lambda_{jk}, \tau_{jk}^2\right) \quad (4)$$

$$\varepsilon_{ij} \sim N\left(0, \sigma_j^2\right) \quad (5)$$

where X_{ij} is isotopic signature j ($\delta^{15}N$-NO_3^- and $\triangle^{17}O$-NO_3^-) of the river water sample i (i = 1, 2, 3…N); S_{jk} denotes the potential NO_3^--N source k (e.g., municipal sewage, soil nitrogen, nitrogen fertilizer and atmospheric nitrate deposition) of isotope j; P_k represents the estimated proportional contribution of source k, which obeys a Dirichlet distribution; C_{jk} refers to the isotopic fractionation associated with nitrogen-cycling processes (e.g., denitrification) for isotope j of source k; and ε_{ij} is the residual error, which represents the unquantified variation among individual mixtures. Additional details concerning the application of this modeling approach can be found in Yang et al. (2013) and Gibrilla et al. (2020). In the current study, the SIAR model was implemented on the R 3.1.2 software, and the modeling protocol used iterations =

500,000, burn-in = 50,000, and iteration maintainer = 30,000. The isotopic signatures of potential nitrate sources considered in this study are summarized in Table 1. Specifically, the $\delta^{15}N$ values for AD, NF, SN, and MS were set as − 2.71 ± 1.67‰, −2.25 ± 1.75‰, 5.04 ± 1.85‰, and 10.49 ± 4.53‰, respectively; corresponding $\triangle^{17}O$ values were 23.80 ± 3.30‰ for AD and − 2.82 ± 1‰ for terrestrial sources such as MS, SN, and NF (see Supplementary Material for details).

3. Results

3.1. Hydrochemical variables and isotopic compositions in surface water

The 13 hydrochemical variables and five stable isotopes obtained from the 17 monitoring sites in the Wen-Rui Tang River network on a monthly basis during April–June 2021 are shown in Table S3 of the Supplementary Material and further summarized in Table 2. DO concentrations varied from 0.71 to 10.05 mg/L, with 72.5%, 25.5%, and 10.0% of the samples meeting the class V (≥2 mg/L, unfavorable for denitrification), class III (≥5 mg/L), and class I (≥7.5 mg/L) water quality standard of China, respectively. Environmental quality standards for surface water in China (GB 3838, 2002) (State Environment Protection Bureau of China, 2002) are described in Table S4. The pH values ranged from 7.35 to 8.68, which indicated that the surface waters were neutral-to-weakly alkaline. Electrical conductivity ($EC_{25\ ^\circ C}$) denotes the amount of dissolved ions. In this study, $EC_{25\ ^\circ C}$ ranged from 100 to 650 μS/cm, which implied relatively dilute ion concentrations. Chlorophyll *a* (Chla) exhibited wide spatio-temporal variations from 0.8 to 118.1 μg/L, with an average value of 12.1 μg/L.

TN concentrations varied from 1.27 to 12.51 mg/L, with nearly all samples (~95%) exceeding the class V water quality standard of 2 mg/L. Spatially, TN concentrations decreased in the following order: sampling sites located at tributaries in old urban area (sites 5, 11, 12, and 17) and old industry zone (site 4) of Wenzhou City > sites located at new urban zone (sites 14 and 15), mainstream (sites 1, 2, 3, 7, 9, and 13), upstream (sites 6 and 8), and wetland (site 16) > site located at river segment for swimming (site 10). The high TN concentrations were found at site 17, reaching 12.51, 8.91, and 9.83 mg/L in April, May, and June 2021, respectively. By contrast, the lowest TN concentration (1.27 mg/L) was observed at site 10 due to that this river segment was severed as a swimming river for residents and was thus well protected by local government. The spatio-temporal variations of NH_4^+-N concentrations were similar to those of TN. The average NH_4^+-N concentration was 2.71 ± 2.63 mg/L (range = 0.20–11.45 mg/L), with > 40% and ~ 80% of the samples exceeding class V (2 mg/L) and class III (1 mg/L) water quality standards, respectively. The NO_3^--N concentrations (mean = 1.87 ± 1.33 mg/L; range = 0.004–5.45 mg/L) were generally lower than NH_4^+-N, constituting ~ 40% of TN concentration on average. The NO_3^--N concentrations were generally higher in the mainstream, upstream, and wetland areas than those in tributaries of old urban area, with the highest value at site 2 in June and lowest value at site 12 in June. The NO_2^--N concentrations (mean = 0.10 ± 0.06 mg/L) were much lower than the NH_4^+-N and NO_3^--N concentrations because of its unstable redox characteristics in most natural waters. Therefore, NO_2^--N had a minimal impact on the isotopic characteristics of NO_3^--N. Mean values of TP and PO_4^{3-}-P were 0.28 ± 0.23 and 0.19 ± 0.19 mg/L, respectively, with ~ 85%, ~50%, and 8% of the samples meeting the class V, class III, and class II water quality standard of 0.4 mg/L, 0.2 mg/L, and 0.1 mg/L for TP, respectively. TP and PO_4^{3-}-P concentrations showed similar spatio-temporal variations to those of TN. TOC concentrations ranged from 1.1 to 12.3 mg/L (mean = 4.0 ± 2.1 mg/L), and Cl^- concentrations ranged from 7.4 to 58.3 mg/L (mean = 27.2 ± 13.1 mg/L). Overall, these results identify that nitrogen pollution was the most serious surface water impairment in the Wen-Rui Tang River network.

The δD and $\delta^{18}O$-H_2O values in surface water of the Wen-Rui Tang River were from − 36.01‰ to − 15.54‰ (average = − 25.99 ± 5.14‰) and − 6.32‰ to − 3.14‰ (average = − 5.11 ± 0.64‰), respectively. The $\delta^{15}N$-NO_3^- in surface water fluctuated from 2.72‰ to 17.72‰ (average = 8.91 ± 3.20‰), with ~ 90% and ~ 50% of the samples exceeding the $\delta^{15}N$ boundaries of NF (6‰) and SN (8‰), respectively. $\delta^{18}O$-NO_3^- in surface water ranged from − 9.36‰ to 35.99‰ with a mean value of 7.36 ± 9.27‰. Most of the $\delta^{18}O$-NO_3^- values concentrated within − 5‰ to 15‰ which represented the theoretical range of $\delta^{18}O$-NO_3^- formed from nitrification. The range of $\triangle^{17}O$-NO_3^- was narrower than that of $\delta^{18}O$-NO_3^-, and it ranged from − 2.82‰ to 9.66‰ (average = 1.06 ± 2.28‰). The highest $\triangle^{17}O$-NO_3^- was observed at site 2 in June, while the lowest value was found at site 7 in April.

Table 1
Average isotopic values and standard deviations for the four potential nitrate sources considered for the Wen-Rui Tang River watershed.

Source	Sampling time	$\delta^{15}N$ (‰)		$\triangle^{17}O$ (‰)	
		Mean	SD[a]	Mean	SD[a]
Precipitation nitrate	April-June 2021	−2.71	1.67	23.80	3.30
Nitrogen fertilizer[b]	December 2020	−2.25	1.75	−2.82[c]	1.00[d]
Soil nitrogen	December 2020	5.04	1.85	−2.82[c]	1.00[d]
Municipal sewage	—	10.49[e]	4.53[e]	−2.82[c]	1.00[d]

[a] SD denotes standard deviation.
[b] Ammonia-based composite fertilizers and urea.
[c] Set as the minimum value for $\triangle^{17}O$-NO_3^- in river water.
[d] Set as doubled the value of analytic precision (Xia et al., 2019).
[e] Data from nearby Changle River watershed (~160 km to the north; Ji et al., 2017).

Table 2
Statistical summary of hydro-chemical variables and isotopic compositions for river water samples from the Wen-Rui Tang River watershed.

Parameters	Number	Mean	SD[a]	Minimum	Maximum	CV (%)[b]
T (°C)	51	23.1	2.9	18.2	28.5	12.4
DO (mg/L)	51	3.68	2.31	0.71	10.05	62.9
pH	51	7.75	0.25	7.35	8.68	3.3
$EC_{25\ ^\circ C}$ (μS/cm)	51	350	120	100	650	34.6
Chla (μg/L)	51	12.1	23.6	0.8	118.1	194.6
TN (mg/L)	51	4.67	2.31	1.27	12.51	49.4
NH_4^+-N (mg/L)	51	2.71	2.63	0.20	11.45	97.2
NO_3^--N (mg/L)	51	1.87	1.33	0.004	5.45	70.9
NO_2^--N (mg/L)	51	0.10	0.06	0.01	0.44	65.6
TP (mg/L)	51	0.28	0.23	0.08	1.32	82.7
PO_4^{3-}-P (mg/L)	51	0.19	0.19	0.02	0.95	99.6
TOC (mg/L)	51	4.0	2.1	1.1	12.3	52.8
Cl^- (mg/L)	51	27.2	13.1	7.4	58.3	48.1
δD (‰)	51	−25.99	5.14	−36.01	−15.54	19.8
$\delta^{18}O$-H_2O (‰)	51	−5.11	0.64	−6.32	−3.14	12.6
$\delta^{15}N$-NO_3^- (‰)	51[c,d]	8.91	3.20	2.72	17.72	35.9
$\delta^{18}O$-NO_3^- (‰)	51[c]	7.36	9.27	−9.36	35.99	126.0
$\triangle^{17}O$-NO_3^- (‰)	51[c]	1.06	2.28	−2.82	9.66	216.2

[a] SD denotes standard deviation.
[b] CV denotes coefficient of variation.
[c] Six samples did not produce N_2O during the bacteria denitrifier method.
[d] One sample is outlier.

3.2. Nitrogen concentrations and isotopic compositions in atmospheric precipitation

The values of nitrogen (TN, NH_4^+-N, NO_2^--N, and NO_3^--N) and isotopic parameters in rainwater samples are shown in Table S5 of the

Supplementary Material and summarized in Table 3. During the study period, TN concentrations showed high spatial and temporal variations, ranging from 0.16 to 6.58 mg/L (average = 1.71 ± 1.25 mg/L). Dissolved inorganic nitrogen (NH_4^+-N + NO_2^--N + NO_3^--N) was the main form of nitrogen in precipitation, accounting for > 80% of the TN concentration. Concentrations of NH_4^+-N ranged from 0.13 to 3.06 mg/L (mean = 0.74 ± 0.58 mg/L) and NO_3^--N from 0.11 to 2.12 mg/L (mean = 0.64 ± 0.49 mg/L). By contrast, NO_2^--N concentrations were much lower (range = <0.003–0.05 mg/L).

During the study period, δD-H_2O values in precipitation ranged from − 76.60‰ to − 4.51‰ (mean = − 38.00 ± 25.70‰) and δ^{18}O-H_2O values from − 10.99‰ to − 2.39‰ (mean = − 6.41 ± 3.08‰). The δ^{15}N-NO_3^- values in precipitation fluctuated from − 5.98‰ to − 0.05‰ with a mean value of − 2.71 ± 1.67‰, and δ^{18}O-NO_3^- ranged from 42.70‰ to 94.92‰ with a mean value of 72.55 ± 11.01‰. In comparison with δ^{18}O-NO_3^-, the $\triangle^{17}$O-NO_3^- in precipitation had narrower ranges of 14.83‰ to 31.39‰, which was higher than those found in groundwater from the Yellow River basin by Liu et al (2013) (range = 7.8–23.3‰), but it was comparable to those of surface waters reported by other studies, such as Hundey et al. (2016) (range = 15.0–30.7‰; Uinta Mountains, Utah, USA) and Huang et al. (2020) (range = 18.3–32.7‰; headwater region of Hun River, northeast China). The narrow range of $\triangle^{17}$O-NO_3^- values is beneficial for separating atmospheric-derived nitrate from microbially produced nitrate, which provides more conclusive discrimination of nitrate sources in surface waters and groundwater. In addition, relatively moderate to significant spatio-temporal variations were found in the nitrogen concentrations and isotope (δ^{15}N/δ^{18}O/$\triangle^{17}$O-NO_3^- and δD/δ^{18}O-H_2O) values of precipitation (see Figs. S1–S6 in Supplementary Material), which implied that future works should create long-term (at least two years) precipitation monitoring network considering more sampling sites to obtain representative data.

4. Discussion

4.1. River water sources

Stable hydrogen and oxygen isotopes of water (δD/δ^{18}O-H_2O) in precipitation and river water are widely used for hydrological tracing because they provide climatic and environmental information (Hu et al., 2019; Wallace et al., 2021; Wassenaar et al., 2011). A regression line of the observed δD-H_2O vs. δ^{18}O-H_2O for local rainwater was determined as the local meteoric water line (LMWL). The LMWL (δD-H_2O = δ^{18}O-H_2O + 10, $R = 0.99$, $p < 0.01$) was calculated according to rainwater samples collected within the Wen-Rui Tang River watershed during April–June 2021. The LMWL was similar to that determined for the nearby Yongan watershed (~95 km to the north; δD-H_2O = 7.58δ^{18}O-H_2O + 14.66) and Qiandao Lake watershed (~230 km to the northwest; δD-H_2O = 8.43δ^{18}O-H_2O + 17.46) (Jin et al., 2019; Hu et al. 2020). Herein, a plot of the measured δD-H_2O vs. δ^{18}O-H_2O for river water (n = 51) and LMWL was employed to assess water source dynamics in the Wen-Rui Tang River watershed. Fig. 2 shows the linear relationship between δD-H_2O and δ^{18}O-H_2O in river water ($R = 0.73$, $p < 0.01$), with the slope of the regression line for river water (5.88) lower than the LMWL (8.27). These results were attributed to evapotranspiration taking place within the watershed. The ^{18}O-H_2O becomes more enriched than deuterium during evaporation, which increases the oxygen and hydrogen isotopic values and generates a systematic deviation from the LMWL (Gonfiantini, 1986). Moreover, the scatter of δD-H_2O vs. δ^{18}O-H_2O values generally fell close to LMWL, indicating that recent rainfall served as the main water source in the Wen-Rui Tang River watershed during the study period.

Table 3
Statistical summary of nitrogen concentrations and isotopic compositions for rainwater samples from the Wen-Rui Tang River watershed.

Parameters	Number	Mean	SD[a]	Minimum	Maximum	CV (%)[b]
TN (mg/L)	38	1.71	1.25	0.16	6.58	73.0
NH_4^+-N (mg/L)	38	0.74	0.58	0.13	3.06	78.4
NO_3^--N (mg/L)	38	0.64	0.49	0.11	2.12	76.6
NO_2^--N (mg/L)	38	0.02	0.01	<0.003	0.05	58.3
δD (‰)	24	−38.00	25.70	−76.60	−4.51	67.6
δ^{18}O-H_2O (‰)	24	−6.41	3.08	−10.99	−2.39	48.1
δ^{15}N-NO_3^- (‰)	24[c,d]	−2.71	1.67	−5.98	−0.05	57.1
δ^{18}O-NO_3^- (‰)	24[c]	72.55	11.01	42.70	94.92	15.2
$\triangle^{17}$O-NO_3^- (‰)	24[c]	23.80	3.33	14.83	31.39	14.0

[a] SD denotes standard deviation.
[b] CV denotes coefficient of variation.
[c] Two samples did not produce N_2O during the bacteria denitrifier method.
[d] Three data points are outliers.

4.2. Nitrogen transformation processes

We used δ^{15}N/δ^{18}O-NO_3^- to provide evidence for major nitrogen-cycling processes (e.g., nitrification and denitrification) controlling NO_3^--N concentrations in the Wen-Rui Tang River watershed (Yang and Toor, 2016; Li et al., 2019). Nitrification is a multi-step process of oxidizing NH_4^+-N to NO_2^--N and then NO_2^--N to NO_3^--N. In theory, nitrifying bacteria produce NO_3^--N by utilizing one oxygen atom from oxygen gas in the air and two oxygen atoms from ambient water; thus, the ratio of oxygen incorporation from water and oxygen gas is 2:1 (Wassenaar, 1995; Kendall and McDonnell, 1998; Mayer et al., 2001). In this study, considering δ^{18}O value of 23.5‰ for atmospheric oxygen and from − 14.16‰ to − 0.92‰ in ambient water measured at the nearest Global Network of Isotopes in Precipitation monitoring station at Fuzhou (~240 km, International Atomic Energy Association), we estimated that the δ^{18}O-NO_3^- values from nitrification should vary from − 1.61‰ to 12.22‰ based on δ^{18}O-NO_3^- = 2 × [δ^{18}O-H2O]/3 + 1 × [δ^{18}O-O2]/3. We also considered that the δ^{18}O values of microbially formed nitrate may be up to 5‰ higher than the calculated theoretical maximum value (Xue et al., 2009). Accordingly, the theoretical δ^{18}O-NO_3^- values for the Wen-Rui Tang River watershed derived from microbial nitrification were calculated to fall within the range of − 1.61‰ to 12.22‰. As

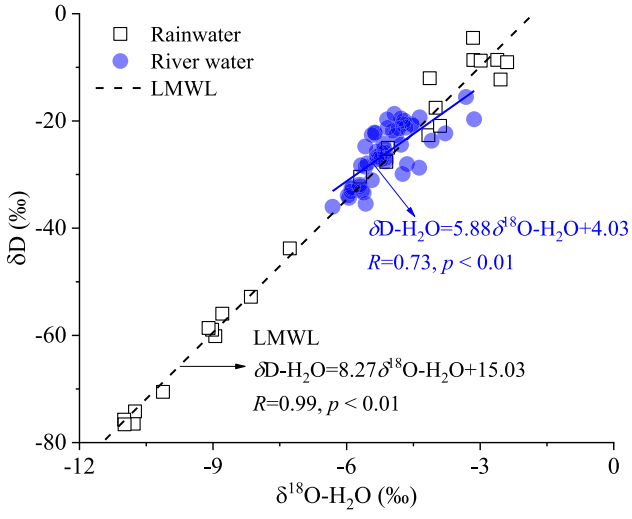

Fig. 2. δD-H_2O and δ^{18}O-H_2O of rainfall and river water in Wen-Rui Tang River watershed plotted along with the Local Meteoric Water Line (LMWL).

shown in Fig. 3, most δ^{18}O-NO_3^- values fell into the theoretical nitrification range in the Wen-Rui Tang River watershed. This result demonstrated that nitrification was a dominant nitrogen transformation process in the Wen-Rui Tang River watershed. Further, these findings suggest that the riverine nitrate mainly formed from the nitrification of nitrogen originating from NF, SN, and MS.

Denitrification is an important microbially facilitated pathway for removing NO_3^--N from aquatic ecosystems under anoxic/hypoxic conditions (DO < 2 mg/L) by reducing NO_3^--N into dinitrogen (N_2), with NO_2^--N, nitric oxide (NO), and N_2O as intermediate products (Hinshaw et al., 2020). During denitrification of NO_3^--N, anaerobic microbes preferentially consume the light isotopes of NO_3^--N (i.e., ^{14}N and ^{16}O), resulting in simultaneous enrichment of ^{15}N and ^{18}O in the residual NO_3^--N fraction along a ~ 2:1 linear line as NO_3^--N concentrations decrease (Nestler et al., 2011; Yue et al., 2014). That is, a significant positive relationship between δ^{15}N-NO_3^- and δ^{18}O-NO_3^- with the slope of regression line being ~ 0.5 as well as a significant negative relationship between δ^{15}N-NO_3^- and NO_3^--N concentrations frequently serve as a denitrification diagnostic in water systems. Fig. 3 shows that the expected positive relationship between δ^{15}N-NO_3^- and δ^{18}O-NO_3^- with slope value of ~ 0.5 was not found in April ($R = -0.48$, $p = 0.098$, slope value = −1.51), May ($R = -0.84$, $p < 0.01$, slope value = −2.26) and June ($R = -0.85$, $p < 0.01$, slope value = −1.64). Additionally, there was no significant negative linear correlation between δ^{15}N-NO_3^- and nitrate concentration in April ($R = 0.023$, $p = 0.94$), May ($R = -0.07$, $p = 0.79$) and June ($R = 0.38$, $p = 0.19$). Consequently, we inferred that denitrification was an insignificant process controlling isotopic compositions of NO_3^--N in surface water of the Wen-Rui Tang River during the study period. This finding is consistent with the generally aerobic conditions (mean DO = 3.68 ± 2.31 mg/L) within the surface waters, which restricts the anaerobic denitrification process.

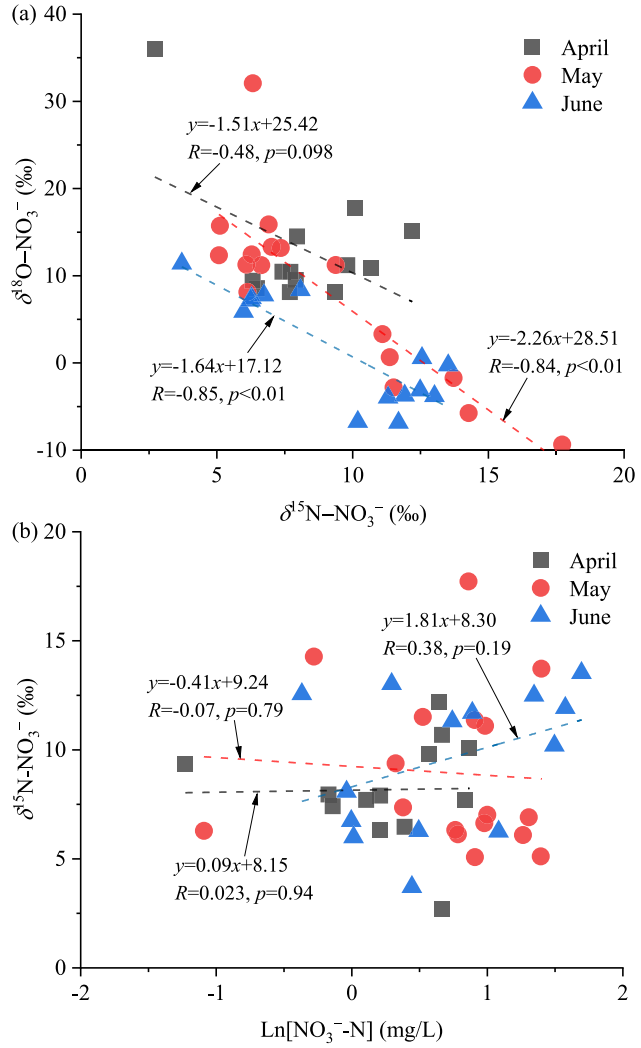

Fig. 3. (a) δ^{15}N-NO_3^- vs. δ^{18}O-NO_3^- and (b) δ^{15}N-NO_3^- vs. NO_3^--N concentrations for river waters in the Wen-Rui Tang River watershed.

4.3. Sources of nitrate

Chloride is generally considered a conservative constituent in natural waters that is not changed through physical, chemical or microbiological processes. Thus, Cl^- is often used as an effective indicator of mixing of different NO_3^--N sources (Widory et al., 2004; Xi et al., 2015; Javadinejad et al., 2019; Bertrand et al., 2022). For instance, high Cl^- concentrations are often found in human/livestock waste, whereas mineral fertilizers generally have high NO_3^--N contents and low Cl^- contents (Liu et al., 2006). Thus, we utilized the molar ratio of Cl^- versus NO_3^--N/Cl^- to obtain more information on pollution source identification. Most of our river samples (especially samples in April) had high Cl^- and low NO_3^--N/Cl^-, which indicated that municipal and livestock sewage were the likely sources of riverine NO_3^--N (Fig. 4).

To obtain qualitative information regarding predominant pollutant sources affecting nitrate concentrations in the river network, we utilized a dual isotope (δ^{15}N, $\triangle^{17}$O-NO_3^-) plot approach. Herein, we assumed that the sources of riverine nitrate in the Wen-Rui Tang River watershed included a combination of AD, NF, SN, and MS (livestock numbers are low within the watershed due to the strict ban of livestock/poultry breeding farms). As shown in Fig. 5, most sampling points for δ^{15}N-NO_3^- vs. $\triangle^{17}$O-NO_3^- distributed in the MS field, whereas 8 points including 5 points in June fell between the AD and terrestrial source fields. This assessment implies that MS was likely a predominant nitrate source, and AD also contributed to the riverine nitrate loads in the Wen-Rui Tang River.

With the purpose of analyzing the relative importance of different nitrate sources, most efforts were focused on applications of SIAR model based on δ^{15}N/δ^{18}O-NO_3^- (Yue et al., 2014; Nyilitya et al., 2021). In this study, we implemented a SIAR model based on δ^{15}N/$\triangle^{17}$O-NO_3^- for the first time in eastern China to provide a quantitative estimate for the probability distribution of the proportional contributions of nitrate from four potential sources (i.e., AD, SN, NF, and MS). The SIAR modeling estimated that MS, SN, AD, and NF contributed 50.5 ± 11.7%, 23.8 ± 13.7%, 14.3 ± 2.9%, and 11.4 ± 8.7% of riverine nitrate, respectively, in the Wen-Rui Tang River watershed (Fig. 6). Overall, MS was the

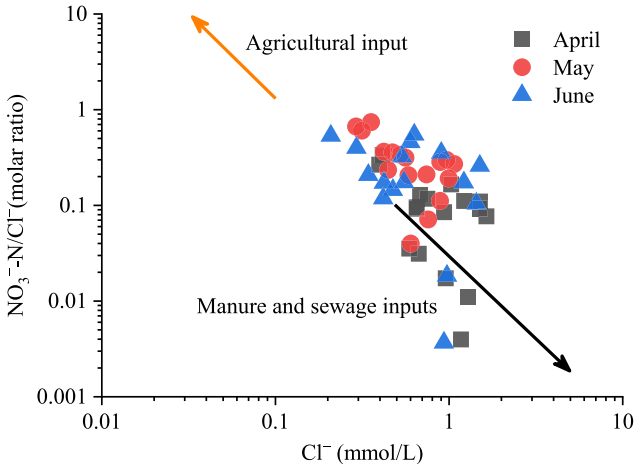

Fig. 4. Correlation between NO_3^--N/Cl^- molar ratio and Cl^- molar concentration as an indicator of agricultural versus manure and municipal sewage inputs.

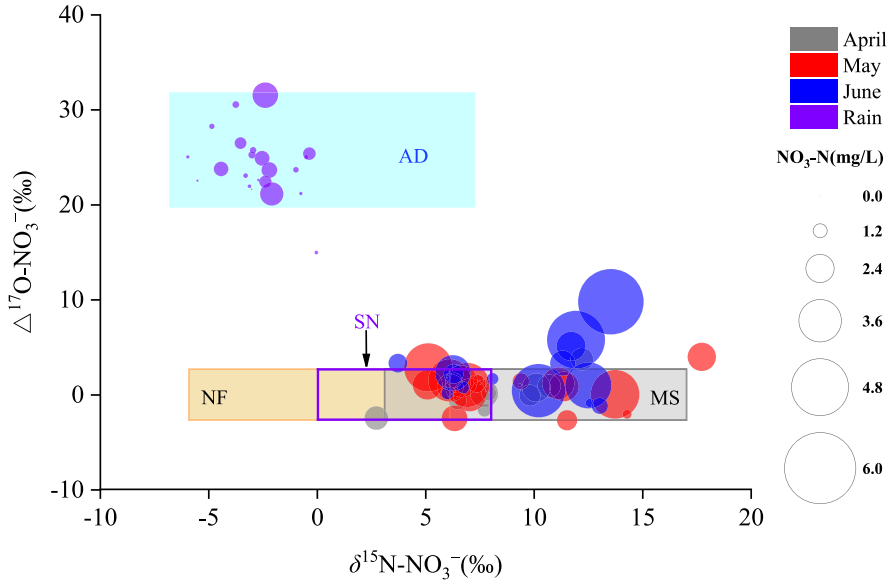

Fig. 5. Scatter plot of δ^{15}N-NO_3^- and $\triangle^{17}$O-NO_3^- values in river water, rainwater and potential nitrate sources in the Wen-Rui Tang River watershed. AD: atmospheric deposition nitrate, NF: nitrogen fertilizer (ammonia-based composite fertilizers and urea); SN: soil nitrogen; MS: municipal sewage.

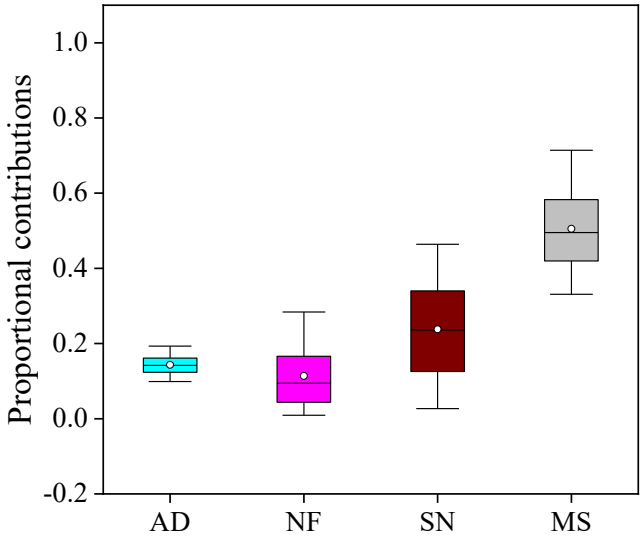

Fig. 6. Proportional contributions from potential nitrate sources based on SIAR model of δ^{15}N/$\triangle^{17}$O-NO_3^-. *Box plots* illustrate the 25th, 50th, and 75th percentiles; the *whiskers* represent the 5th and 95th percentiles; the *small white circles* denote the mean value. AD: atmospheric deposition nitrate; NF: nitrogen fertilizer (ammonia-based composite fertilizers and urea); SN: soil nitrogen; MS: municipal sewage.

greatest nitrate contributor, which was in good agreement with the qualitative results from the dual stable isotope and hydrochemical (e.g., Cl^- content) assessments. Notably, AD accounted for 14.3 ± 2.9% of riverine nitrate, indicating the importance of considering atmospheric nitrate inputs to coastal plain river networks of eastern China. The AD nitrate input is expedited by low soil infiltration in residential/urban areas where impervious surfaces and storm runoff events during the wet season result in rapid transport of runoff waters into the river network. Notably, in this study, river water and rainwater samples collected during the wet season were assumed to reflect the riverine nitrate with the influence of precipitation and terrestrial pollution sources. Owing to the low or no precipitation during the dry season, sampling campaigns were not carried out. It appears that the contribution of MS might increase while that of NF, SN, and AD might decrease sharply during the dry season due to the less precipitation and few leaching effects of NF and SN. Considering lack of dilution effect of precipitation, the nitrate concentration in the Wen-Rui Tang River network during the dry season might be higher than that during the wet season (Ji et al., 2016).

This study identified MS as the predominant source of riverine nitrate in the Wen-Rui Tang River network. Despite recent efforts to collect and conveyed all wastewater to central wastewater treatment plants, a certain amount of municipal sewage appears to enter the nearby river *via* sewer overflow caused by storm flow, as well as leaking sewer systems in parts of the study region. Therefore, urban sewage collection and pipeline networks should be improved to assure effective collection of sewage. Further, an adequate stormwater system is necessary to prevent municipal sewage mixing with stormwater runoff during storm events (e.g., typhoons). SN and NF were also identified as important nitrate sources. Hence, enhancing nitrogen fertilizer-use efficiency utilizing the 4R (right source, rate, time, and place) nutrient stewardship initiative would be a practical method to reduce nitrogen fertilizer leaching. Finally, AD was identified as an important contributor of nitrate to the Wen-Rui Tang River network. With continuing improvements to domestic sewage treatment processing capacity/efficiency and decreasing fertilizer application rates in China, the relative contribution of the AD nitrate source to the Wen-Rui Tang River is expected to increase in the future. Incorporating "sponge city" management practices to reduce direct runoff and promote infiltration can significantly reduce nitrate transport and facilitate nitrate losses (e.g., plant utilization and denitrification along groundwater pathways). Furthermore, the use of green infrastructure, such as bioswales, riparian plantings, and buffer strips, may provide additional opportunities to attenuate riverine nitrate contributions from AD, NF, SN, and MS before these waters/nutrients enter the coastal plain river network.

4.4. Uncertainty analysis

An uncertainty index (UI_{90}), presented by Ji et al. (2017), was calculated to characterize the degree of uncertainty associated with the apportionment results of the δ^{15}N/$\triangle^{17}$O-NO_3^- method. UI_{90} denotes the difference in the proportional contribution between the 5% and 95% quantiles divided by 0.9 (see detailed information in Shang et al., 2020; Torres-Martínez et al., 2021a, 2021b; Ju et al., 2022). A small UI_{90}

demonstrates that the source contribution is quite stable, whereas large values indicate strong variability in the source contribution. As shown in Fig. 7, AD contributions were relatively stable, displaying a UI_{90} of 0.105, whereas the strongest uncertainty was associated with SN (UI_{90} = 0.486). MS and NF exhibited moderate uncertainties, with UI_{90} values of 0.426 for MS and 0.305 for NF. The increased uncertainty for SN and MS may be attributed to the inherent spatio-temporal variations for the isotopic composition of these sources. More rigorous investigation on the spatio-temporal variations in the isotopic composition of these nitrate pollution sources and determination of the isotopic fractionation factor during the biochemical processes are important to further reduce the uncertainties for enhancing the quantitative apportionment of nitrate sources. In addition, as suggested by Ju et al. (2022), future works should focus on incorporating extraneous information associated with the natural distribution of the input parameters and then extracting the covariate information if a strong factor that causes a pseudo-replicate in mixture samples exists.

5. Conclusions

We used environmental isotopes in combination with water chemistry characteristics to identify nitrate sources and transformations in a typical coastal plain river network in eastern China. The novelty of this study is the application of $\triangle^{17}O\text{-}NO_3^-$ to identify riverine nitrate sources in eastern China for the first time. Nitrate was a major pollutant contributing to water quality degradation (e.g., eutrophication, hypoxia/anoxia) in the Wen-Rui Tang River watershed. The nitrate concentrations varied from 0.004 to 5.45 mg/L with an average value of 1.87 ± 1.33 mg/L during the study period. $\delta D\text{-}H_2O$ and $\delta^{18}O\text{-}H_2O$ compositions indicated that river water primarily consisted of modern/recent precipitation, with minor alteration by evaporation. The $\delta^{15}N/\delta^{18}O\text{-}NO_3^-$ values revealed no detectable denitrification, whereas nitrification was revealed as a predominant nitrogen-cycling process. The $\triangle^{17}O\text{-}NO_3^-$ values in river water and rainwater of the Wen-Rui Tang River watershed ranged from − 2.82‰ to 9.66‰ and from 14.83‰ to 31.39‰, respectively. The SIAR model based on $\delta^{15}N/\triangle^{17}O\text{-}NO_3^-$ provided apportionment for the proportional contributions of potential pollution sources (AD, NF, SN, and MS). The SIAR modeling results indicated that MS (50.5 ± 11.7%) was the dominant source of nitrate, followed by SN (23.8 ± 13.7%), AD (14.3 ± 2.9%), and NF (11.4 ± 8.7%). The uncertainty analysis identified the greatest uncertainty for SN (UI_{90} = 0.486), followed by MS (UI_{90} = 0.426), NF (UI_{90} = 0.305), and AD (UI_{90} = 0.105). Notably, the $\triangle^{17}O\text{-}NO_3^-$ values for precipitation and river water provided the first quantitative estimate for AD, revealing AD as an important nitrate source for rivers in eastern China, a region experiencing high inputs of atmospheric nitrogen deposition.

Overall, the results showed that $\triangle^{17}O\text{-}NO_3^-$ was more effective than $\delta^{18}O\text{-}NO_3^-$ for enhancing riverine nitrate pollution source apportionment, especially for the identification of atmospheric nitrate contribution. The reasons are as follows: (1) $\triangle^{17}O\text{-}NO_3^-$ values are stable and cannot be changed during the nitrogen biogeochemical transformation processes occurring in the terrestrial systems. Conversely, the initial $\delta^{18}O\text{-}NO_3^-$ values of AD might be altered by ^{18}O fractionation during nitrogen cycling and thereby blur the estimation results; (2) the isotopic range of $\triangle^{17}O\text{-}NO_3^-$ in AD is narrower than that of $\delta^{18}O\text{-}NO_3^-$, which is beneficial to reinforce the accuracy of the nitrate source apportionment results. The results of this study can have significant implications for local water resource managers because they can develop effective target nutrient control and remediation strategies at the watershed scale with quantitative information regarding riverine nitrate sources. Future studies should exploit long-term and high-frequency sampling regimes covering different climate and hydrological conditions, which could provide detailed information regarding nitrogen discharge patterns related to human activities, climate conditions, watershed hydrology, and seasonality, and thus further improve our understanding of riverine nitrate pollution sources.

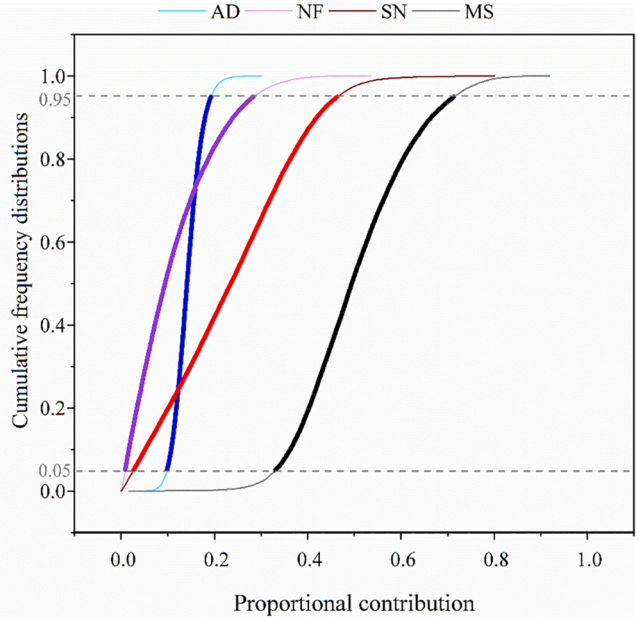

Fig. 7. Cumulative probability distributions for proportional contributions from AD, NF, SN and MS nitrate sources based on SIAR model using $\delta^{15}N/\triangle^{17}O\text{-}NO_3^-$. AD: atmospheric deposition nitrate; NF: nitrogen fertilizer (ammonia-based composite fertilizers and urea); SN: soil nitrogen; MS: municipal sewage.

6. Ethical Approvalss

Not applicable.

7. Consent to Participate

Not applicable.

8. Consent to Publish

Not applicable.

9. Fundingss

This work was funded by the National Natural Science Foundation of China (Grant No. 51979197), Second Tibetan Plateau Scientific Expedition and Research Program (Grant No. 2019QZKK0903), and Science Research Funding of Wenzhou Medical University (Grant No. QTJ18032).

10. Availability of data and materials

All data generated or analyzed during this study are included in this published article.

Declaration of Competing Interest

The authors declare that they have no known competing financial interests or personal relationships that could have appeared to influence the work reported in this paper.

Appendix A. Supplementary data

Supplementary data to this article can be found online at https://doi.org/10.1016/j.jhydrol.2022.127829.

References

Bertrand, G., Petelet-Giraud, E., Cary, L., Hirata, R., Montenegro, S., Paiva, A., Mahlknecht, J., Coelho, V., Almeida, C., 2022. Delineating groundwater contamination risks in southern coastal metropoles through implementation of geochemical and socio-environmental data in decision-tree and geographical information system. Water Res. 209, 117877 https://doi.org/10.1016/j.watres.2021.117877.

Biddau, R., Cidu, R., Pelo, S.D., Carletti, A., Ghiglieri, G., Pittalis, D., 2019. Source and fate of nitrate in contaminated groundwater systems: Assessing spatial and temporal variations by hydrogeochemistry and multiple stable isotope tools. Sci. Total Environ. 647, 1121–1136. https://doi.org/10.1016/j.scitotenv.2018.08.007.

Burow, K.R., Nolan, B.T., Rupert, M.G., Dubrovsky, N.M., 2010. Nitrate in groundwater of the United States, 1991–2003. Environ. Sci. Technol. 44 (13), 4988–4997. https://doi.org/10.1021/es100546y.

Casciotti, K.L., Sigman, D.M., Hastings, M.G., Böhlke, J.K., Hilkert, A., 2002. Measurement of the oxygen isotopic composition of nitrate in seawater and freshwater using the denitrifier method. Anal. Chem. 74 (19), 4905–4912. https://doi.org/10.1021/ac020113w.

Chen, X., Jiang, C., Zheng, L., Dong, X., Chen, Y., Li, C., 2020. Identification of nitrate sources and transformations in basin using dual isotopes and hydrochemistry combined with a Bayesian mixing model: Application in a typical mining city. Environ. Pollut. 267, 115651 https://doi.org/10.1016/j.envpol.2020.115651.

Gibrilla, A., Fianko, J.R., Ganyaglo, S., Adomako, D., Anornu, G., Zakaria, N., 2020. Nitrate contamination and source apportionment in surface and groundwater in Ghana using dual isotopes (^{15}N and ^{18}O-NO_3) and a Bayesian isotope mixing model. J. Contam. Hydrol. 233, 103658 https://doi.org/10.1016/j.jconhyd.2020.103658.

Gonfiantini, R., 1986. Environmental isotopes in lake studies. Handbook of Environmental Isotope Geochemistry; the Terrestrial Environment. Elsevier Science, Amsterdam, pp. 113–168. https://doi.org/10.1016/B978-0-444-42225-5.50008-5.

Hinshaw, S.E., Zhang, T., Harrison, J.A., Dahlgren, R.A., 2020. Excess N_2 and denitrification in hyporheic porewaters and groundwaters of the San Joaquin River, California. Water Res. 168, 115161 https://doi.org/10.1016/j.watres.2019.115161.

Hu, M., Liu, Y., Zhang, Y., Dahlgren, R.A., Chen, D., 2019. Coupling stable isotopes and water chemistry to assess the role of hydrological and biogeochemical processes on riverine nitrogen sources. Water Res. 150, 418–430. https://doi.org/10.1016/j.watres.2018.11.082.

Hu, M., Zhang, Y., Wu, K., Shen, H., Yao, M., Dahlgren, R.A., Chen, D., 2020. Assessment of streamflow components and hydrologic transit times using stable isotopes of oxygen and hydrogen in waters of a subtropical watershed in eastern China. J. Hydrol. 589, 125363 https://doi.org/10.1016/j.jhydrol.2020.125363.

Huang, S., Wang, F., Elliott, E.M., Zhu, F., Zhu, W., Koba, K., Yu, Z., Hobbie, E.A., Michalski, G., Kang, R., Wang, A., Zhu, J., Fu, S., Fang, Y., 2020. Multiyear measurements on $\Delta^{17}O$ of stream nitrate indicate high nitrate production in a temperate forest. Environ. Sci. Technol. 54 (7), 4231–4239. https://doi.org/10.1021/acs.est.9b07839.

Hundey, E.J., Russell, S.D., Longstaffe, F.J., Moser, K.A., 2016. Agriculture causes nitrate fertilization of remote alpine lakes. Nat. Commun. 7, 10571. https://doi.org/10.1038/ncomms10571.

Javadinejad, S., Ostad-Ali-Askari, K., Jafary, F., 2019. Using simulation model to determine the regulation and to optimize the quantity of chlorine injection in water distribution networks. Model. Earth Syst. Environ. 5 (3), 1015–1023. https://doi.org/10.1007/s40808-019-00587-x.

Ji, X.L., Dahlgren, R.A., Zhang, M.H., 2016. Comparison of seven water quality assessment methods for the characterization and management of highly impaired river systems. Environ. Monit. Assess. 188 (1), 15. https://doi.org/10.1007/s10661-015-5016-2.

Ji, X., Xie, R., Hao, Y., Lu, J., 2017. Quantitative identification of nitrate pollution sources and uncertainty analysis based on dual isotope approach in an agricultural watershed. Environ. Pollut. 229, 586–594. https://doi.org/10.1016/j.envpol.2017.06.100.

Jin, Z., Cen, J., Hu, Y., Li, L., Shi, Y., Fu, G., Li, F., 2019. Quantifying nitrate sources in a large reservoir for drinking water by using stable isotopes and a Bayesian isotope mixing model. Environ. Sci. Pollut. R. 26 (20), 20364–20376. https://doi.org/10.1007/s11356-019-05296-7.

Ju, Y., Mahlknecht, J., Lee, K.K., Kaown, D., 2022. Bayesian approach for simultaneous recognition of contaminant sources in groundwater and surface-water resources. Cur. Opinion Environ. Sci. Health 25, 100321. https://doi.org/10.1016/j.coesh.2021.100321.

Kendall, C., McDonnell, J., 1998. Isotope Tracers in Catchment Hydrology. Elsevier Science, Amsterdam, pp. 519–576.

Li, C., Li, S.L., Yue, F.J., Liu, J., Zhong, J., Yan, Z.F., Zhang, R.C., Wang, Z.J., Xu, S., 2019. Identification of sources and transformations of nitrate in the Xijiang River using nitrate isotopes and Bayesian model. Sci. Total Environ. 646, 801–810. https://doi.org/10.1016/j.scitotenv.2018.07.345.

Liao, Z., Li, P., Shang, X., 2015. Difference between urban and rural of atmospheric nitrogen and phosphorus deposition in typical areas of Wenzhou. Zhejiang Agr. Sci. 56 (1), 123–126. (in Chinese). https://doi.org/10.16178/j.issn.0528-9017.20150140.

Liao, Z., Ji, X., Ma, Y., Lv, B., Huang, W., Zhu, X., Fang, M., Wang, Q., Wang, X., Dahlgren, R., Shang, X., 2021. Airborne microplastics in indoor and outdoor environments of a coastal city in Eastern China. J. Hazard. Mater. 417, 126007 https://doi.org/10.1016/j.jhazmat.2021.126007.

Liu, L., Zhang, X., Wang, S., Lu, X., Ouyang, X., 2016. A review of spatial variation of inorganic nitrogen (N) wet deposition in China. PLoS ONE 11 (1), e0146051. https://doi.org/10.1371/journal.pone.0146051.

Liu, C.Q., Li, S.L., Lang, Y.C., Xiao, H.Y., 2006. Using $\delta^{15}N$ and $\delta^{18}O$ values to identify nitrate sources in karst ground water, Guiyang. Southwest China. Environ. Sci. Technol. 40 (22), 6928–6933. https://doi.org/10.1021/es0610129.

Liu, T., Wang, F., Michalski, G., Xia, X., Liu, S., 2013. Using ^{15}N, ^{17}O, and ^{18}O to determine nitrate sources in the Yellow River, China. Environ. Sci. Technol. 47 (23), 13412–13421. https://doi.org/10.1021/es403357m.

Mayer, B., Bollwerk, S.M., Mansfeldt, T., Hutter, B., Veizer, J., 2001. The oxygen isotope composition of nitrate generated by nitrification in acid forest floors. Geochim. Cosmochim. Acta 65 (16), 2743–2756. https://doi.org/10.1016/S0016-7037(01)00612-3.

Michalski, G., Scott, Z., Kabiling, M., Thiemens, M.H., 2003. First measurements and modeling of $\Delta^{17}O$ in atmospheric nitrate. Geophys. Res. Lett. 30 (16), 141–144. https:// doi.org/10.1029/2003gl017015.

Michalski, G., Meixner, T., Fenn, M., Hernandez, L., Sirulnik, A., Allen, E., Thiemens, M., 2004. Tracing atmospheric nitrate deposition in a complex semiarid ecosystem using $\Delta^{17}O$. Environ. Sci. Technol. 38 (7), 2175–2181. https://doi.org/10.1021/es034980+.

Narvaez-Montoya, C., Torres-Martínez, J.A., Pino-Vargas, E., Cabrera-Olivera, F., Loge, F.J., Mahlknecht, J., 2022. Predicting adverse scenarios for a transboundary coastal aquifer system in the Atacama Desert (Peru/Chile). Sci. Total Environ. 806, 150386 https://doi.org/10.1016/j.scitotenv.2021.150386.

Nestler, A., Berglund, M., Accoe, F., Duta, S., Xue, D., Boeckx, P., Taylor, P., 2011. Isotopes for improved management of nitrate pollution in aqueous resources: review of surface water field studies. Environ. Sci. Pollut. R. 18 (4), 519–533. https://doi.org/10.1007/s11356-010-0422-z.

Nyilitya, B., Mureithi, S., Bauters, M., Boeckx, P., 2021. Nitrate source apportionment in the complex Nyando tropical river basin in Kenya. J. Hydrol. 594, 125926 https://doi.org/10.1016/j.jhydrol.2020.125926.

Ostad-Ali-Askari, K., Shayannejad, M., Ghorbanizadeh-Kharazi, H., 2017. Artificial neural network for modeling nitrate pollution of groundwater in marginal area of Zayandeh-rood River, Isfahan. Iran. Ksce J. Civ. Eng. 21 (1), 134–140. https://doi.org/10.1007/s12205-016-0572-8.

Ostad-Ali-Askari, K., Shayannejad, M., 2021. Quantity and quality modelling of groundwater to manage water resources in Isfahan-Borkhar Aquifer. Environ. Dev. Sustain. 23 (11), 15943–15959. https://doi.org/10.1007/s10668-021-01323-1.

Ostad-Ali-Askari, K., Ghorbanizadeh Kharazi, H., Shayannejad, M., Zareian, M.J., 2019. Effect of management strategies on reducing negative impacts of climate change on water resources of the Isfahan-Borkhar aquifer using MODFLOW. River Res. Appl. 35 (6), 611–631. https://doi.org/10.1002/rra.3463.

Panagopoulos, A., 2021. Techno-economic assessment of Minimal Liquid Discharge (MLD) treatment systems for saline wastewater (brine) management and treatment. Process Saf. Environ. 146, 656–669. https://doi.org/10.1016/j.psep.2020.12.007.

Panagopoulos, A., 2022. Study and evaluation of the characteristics of saline wastewater (brine) produced by desalination and industrial plants. Environ. Sci. Pollut. Res. 29 (16), 23736–23749. https://doi.org/10.1007/s11356-021-17694-x.

Paredes, I., Otero, N., Soler, A., Green, A.J., Soto, D.X., 2020. Agricultural and urban delivered nitrate pollution input to Mediterranean temporary freshwaters. Agric. Ecosyst. Environ. 294, 106859 https://doi.org/10.1016/j.agee.2020.106859.

Parnell, A.C., Inger, R., Bearhop, S., Jackson, A.L., 2010. Source partitioning using stable isotopes: coping with too much variation. PLoS ONE 5 (3), e9672. https://doi.org/10.1371/journal.pone.0009672.

Shang, X., Huang, H., Mei, K., Xia, F., Chen, Z., Yang, Y., Dahlgren, R.A., Zhang, M.H., Ji, X.L., 2020. Riverine nitrate source apportionment using dual stable isotopes in a drinking water source watershed of southeast China. Sci. Total Environ. 724, 137975 https://doi.org/10.1016/j.scitotenv.2020.137975.

Sigman, D.M., Casciotti, K.L., Andreani, M., Barford, C., Galanter, M., Böhlke, J., 2001. A bacterial method for the nitrogen isotopic analysis of nitrate in seawater and freshwater. Anal. Chem. 73 (17), 4145–4153. https://doi.org/10.1021/ac010088e.

State Environment Protection Bureau of China, 2002. Environmental Quality Standards for Surface Water. China Environmental Science Press, Beijing (in Chinese).

Torres-Martínez, J.A., Mora, A., Knappett, P.S.K., Ornelas-Soto, N., Mahlknecht, J., 2020. Tracking nitrate and sulfate sources in groundwater of an urbanized valley using a multi-tracer approach combined with a Bayesian isotope mixing model. Water Res. 182, 115962 https://doi.org/10.1016/j.watres.2020.115962.

Torres-Martínez, J.A., Mora, A., Mahlknecht, J., Daesle, L.W., Cervantes-Aviles, P.A., Ledesma-Ruiz, R., 2021a. Estimation of nitrate pollution sources and transformations in groundwater of an intensive livestock-agricultural area (Comarca Lagunera), combining major ions, stable isotopes and MixSIAR model. Environ. Pollut. 269, 115445 https://doi.org/10.1016/j.envpol.2020.115445.

Torres-Martínez, J.A., Mora, A., Mahlknecht, J., Kaown, D., Barceló, D., 2021b. Determining nitrate and sulfate pollution sources and transformations in a coastal aquifer impacted by seawater intrusion-A multi-isotopic approach combined with self-organizing maps and a Bayesian mixing model. J. Hazard. Mater. 417, 126103 https://doi.org/10.1016/j.jhazmat.2021.126103.

Wallace, S., Biggs, T., Lai, C.T., McMillan, H., 2021. Tracing sources of stormflow and groundwater recharge in an urban, semi-arid watershed using stable isotopes. J. Hydrol.–Reg. Stud. 34, 100806 https://doi.org/10.1016/j.ejrh.2021.100806.

Wassenaar, L.I., 1995. Evaluation of the origin and fate of nitrate in the Abbotsford Aquifer using the isotopes of ^{15}N and ^{18}O in NO_3^-. Appl. Geochem. 10 (4), 391–405. https://doi.org/10.1016/0883-2927(95)00013-A.

Wassenaar, L.I., Athanasopoulos, P., Hendry, M.J., 2011. Isotope hydrology of precipitation, surface and ground waters in the Okanagan Valley, British Columbia. Canada. J. Hydrol. 411 (1–2), 37–48. https://doi.org/10.1016/j.jhydrol.2011.09.032.

Wenzhou Municipal People's Government, 2020. Wenzhou Yearbook. Publishing Hourse of Local Records, Beijing, China in Chinese.

Widory, D., Kloppmann, W., Chery, L., Bonnin, J., Rochdi, H., Guinamant, J.L., 2004. Nitrate in groundwater: an isotopic multi-tracer approach. J. Contam. Hydrol. 72 (1–4), 165–188. https://doi.org/10.1016/j.jconhyd.2003.10.010.

Wu, H., Dong, Y., Gao, L., Song, X., Liu, F., Peng, X., Zhang, G.L., 2021. Identifying nitrate sources in surface water, regolith and groundwater in a subtropical red soil Critical Zone by using dual nitrate isotopes. Catena 198, 104994. https://doi.org/10.1016/j.catena.2020.104994.

Xi, S., Liu, G., Zhou, C., Wu, L., Liu, R., 2015. Assessment of the sources of nitrate in the Chaohu Lake, China, using a nitrogen and oxygen isotopic approach. Environ. Earth Sci. 74 (2), 1647–1655. https://doi.org/10.1007/s12665-015-4170-8.

Xia, X., Li, S., Wang, F., Zhang, S., Fang, Y., Li, J., Michalski, G., Zhang, L., 2019. Triple oxygen isotopic evidence for atmospheric nitrate and its application in source identification for river systems in the Qinghai-Tibetan Plateau. Sci. Total Environ. 688, 270–280. https://doi.org/10.1016/j.scitotenv.2019.06.204.

Xue, D., Botte, J., De Baets, B., Accoe, F., Nestler, A., Taylor, P., Van Cleemput, O., Berglund, M., Boeckx, P., 2009. Present limitations and future prospects of stable isotope methods for nitrate source identification in surface and groundwater. Water Res. 43 (5), 1159–1170. https://doi.org/10.1016/j.watres.2008.12.048.

Yang, L., Han, J., Xue, J., Zeng, L., Shi, J., Wu, L., Jiang, Y., 2013. Nitrate source apportionment in a subtropical watershed using Bayesian model. Sci. Total Environ. 463, 340–347. https://doi.org/10.1016/j.scitotenv.2013.06.021.

Yang, Y.Y., Toor, G.S., 2016. $\delta^{15}N$ and $\delta^{18}O$ reveal the sources of nitrate-nitrogen in urban residential stormwater runoff. Environ. Sci. Technol. 50 (6), 2881–2889. https://doi.org/10.1021/acs.est.5b05353.

Yue, F.J., Liu, C.Q., Li, S.L., Zhao, Z.Q., Liu, X.L., Ding, H., Liu, B.J., Zhong, J., 2014. Analysis of $\delta^{15}N$ and $\delta^{18}O$ to identify nitrate sources and transformations in Songhua River, Northeast China. J. Hydrol. 519, 329–339. https://doi.org/10.1016/j.jhydrol.2014.07.026.

Zhang, Y., Shi, P., Song, J.X., Li, Q., 2019. Application of nitrogen and oxygen isotopes for source and fate identification of nitrate pollution in surface water: a review. Appl. Sci. 9 (1), 18. https://doi.org/10.3390/app9010018.

Zhu, J., He, N., Wang, Q., Yuan, G., Wen, D., Yu, G., Jia, Y., 2015. The composition, spatial patterns, and influencing factors of atmospheric wet nitrogen deposition in Chinese terrestrial ecosystems. Sci. Total Environ. 511, 777–785. https://doi.org/10.1016/j.scitotenv.2014.12.038.